

Quantum synchronization in an optomechanical system based on Lyapunov control

Wenlin Li, Chong Li, and Heshan Song*

School of Physics and Optoelectronic Engineering, Dalian University of Technology, 116024, China

(Received 29 June 2015; revised manuscript received 30 May 2016; published 22 June 2016)

We extend the concepts of quantum complete synchronization and phase synchronization, which were proposed in A. Mari *et al.*, *Phys. Rev. Lett.* **111**, 103605 (2013), to more widespread quantum generalized synchronization. Generalized synchronization can be considered a necessary condition or a more flexible derivative of complete synchronization, and its criterion and synchronization measure are proposed and analyzed in this paper. As examples, we consider two typical generalized synchronizations in a designed optomechanical system. Unlike the effort to construct a special coupling synchronization system, we purposefully design extra control fields based on Lyapunov control theory. We find that the Lyapunov function can adapt to more flexible control objectives, which is more suitable for generalized synchronization control, and the control fields can be achieved simply with a time-variant voltage. Finally, the existence of quantum entanglement in different generalized synchronizations is also discussed.

DOI: [10.1103/PhysRevE.93.062221](https://doi.org/10.1103/PhysRevE.93.062221)**I. INTRODUCTION**

Complete synchronization and phase synchronization between two continuous variable (CV) quantum systems were first studied by Mari *et al.* in a mesoscopic optomechanical system [1], and they also made the forward-looking prediction that quantum synchronization has potential and important applications in quantum-information processing (QIP). Subsequently, quantum synchronization has been explored at length in a variety of quantum systems, such as cavity quantum electrodynamics [2,3], atomic ensembles [4–6], van der Pol (VdP) oscillators [3,7–10], Bose-Einstein condensation [11], superconducting circuit systems [12,13], and so on. In those works, quantum synchronization was extended from a CV system to finite-dimensional Hilbert space corresponding to better quantum properties, and quantum correlation was also analyzed quantitatively in those synchronous quantum systems [3,4,7,14]. In addition, quantum synchronization criteria [4,9,15,16] and synchronization among nodes in a quantum network [17,18] are still hot topics in the field of quantum synchronization theory. In addition to the theoretical research, a series of experiments have demonstrated the existence of synchronization in mesoscopic optomechanical and nanoelectromechanical systems in recent years, and this has provided a reliable platform for the development of quantum synchronization [19–22].

Generally, existing quantum synchronization schemes can be attributed to the concept of coupling synchronization, i.e., one subsystem of the synchronous system plays the role of a controller acting on the other subsystem [1–10,14,15]. A significant advantage of this kind of direct linking is its strong maneuverability. However, there remain some difficulties in achieving better applications in QIP with quantum synchronization. For weak coupling at the quantum level, it is difficult to eliminate the difference between subsystems if the difference is big enough, and in fact this is often the case. Fundamentally, a driving or pump field that is too strong will compel systems to take the form of forced synchronization, as

occurs in previous works [1–4,14]. This deficiency of coupling synchronization is a severe limitation that makes it difficult to achieve other types of synchronization, including complete and phase synchronization. In some previous investigations, regulating the effective potential was a clever way to achieve a multistable synchronization transition from 0-synchronization to π -synchronization between identical subsystems [10,14]. However, the idea of achieving antiphase synchronization and projective synchronization by controlling different subsystems is rarely discussed in the context of quantum systems, even though these synchronizations have been widely applied in the classical field [23–25]. In addition, the effective potential usually causes the synchronization to depend on the initial conditions, and this may be invalid in an array or a network [26]. These characteristics limit the application of multistable coupling synchronization.

In traditional control theory, in addition to the coupling terms, there exists an external controller that is imposed on the response system in order to provide better control capability. This implies that a designed controller can establish a more flexible relationship between two controlled subsystems [27]. It is thought-provoking to consider such problems: can more generalized synchronizations (such as the above-mentioned antiphase and projective synchronizations) be extended and obtained in the quantum domain? If the answer is yes, what kinds of criteria and measures are needed in this quantum generalized synchronization? Most importantly, how are the controllers designed to satisfy various requirements corresponding to different kinds of generalized synchronizations?

To answer the above questions, in this paper we study the general properties of different synchronization forms, and we expand them to quantum mechanics based on Mari's complete synchronization theory. The criteria and measures of generalized synchronization are also proposed, and they will be divided into two orders for the sake of convenient calculation and analysis. Instead of directly establishing interaction between two subsystems, here we utilize Lyapunov control theory (which has exhibited comprehensive applications in target quantum state preparation and suppressing decoherence) to design the external controller [27–29]. The significance of Lyapunov control is that it can be used both in open- and

*hssong@dlut.edu.cn

closed-loop control. Therefore, in quantum control one can always avoid impossible or difficult measures by simulating the control field in advance. Although the Lyapunov function is constituted by expectation values, our results show that the quantum fluctuations can also be effectively subdued by the controller. In addition, classical and quantum correlations are considered by calculating the Lyapunov exponent and Gaussian negativity. In particular, we demonstrate that CV entanglement can exist in generalized synchronization, however it will disappear if generalized synchronization tends to complete synchronization. This phenomenon is consistent with Mari's and Ameri's conclusions about entanglement in complete synchronization [1,3]. Therefore, we believe that existing quantum complete synchronization can be included in our generalized synchronization theory.

This paper is organized as follows: In Sec. II, we introduce the definition and the properties, especially the method of measurement, of quantum generalized synchronization. In Sec. III, we analyze the dynamics of an optomechanical system, and we realize two kinds of representative generalized synchronization (constant error synchronization in Sec. III A and time delay synchronization in Sec. III B) by designing appropriate control fields based on Lyapunov function theory. The correlation in generalized synchronization is also discussed in Sec. IV, and a summary is given in Sec. V.

II. QUANTUM GENERALIZED SYNCHRONIZATION

We begin this section with a brief introduction about generalized synchronization and its expansion in the quantum domain. Consider two general classical dynamics systems whose evolutions satisfy the following equations:

$$\begin{aligned} \partial_t x_1(t) &= F(x_1(t)) + U_{c1}(x_1, x_2) + U_{e1}, \\ \partial_t x_2(t) &= F(x_2(t)) + U_{c2}(x_1, x_2) + U_{e2}, \end{aligned} \quad (1)$$

where $x_{1,2}(t) \in R^n$ are the state variables of two systems at time t . $U_{c1,2}$ are the mutual couplings between systems, and correspondingly $U_{e1,2}$ are the external controllers belonging to their respective systems. If there are continuous mappings $h_1, h_2 : R^n \rightarrow R^k$, and if the synchronization condition in Eq. (2) can be achieved when $t \rightarrow \infty$, then two systems depending on h_1, h_2, x_1 , and x_2 will be of consistent evolution,

$$\lim_{t \rightarrow \infty} |h_1(x_1(t)) - h_2(x_2(t))| \rightarrow 0. \quad (2)$$

This controllable correlation is called generalized synchronization, and it will degenerate to common complete synchronization or phase synchronization upon selecting $h_i(x_i) = x_i$ or $h_i(x_i) = \arg(x_i)$, respectively. Similar to Mari's measure, $S_c(t) := \langle \hat{q}^2(t) + \hat{p}^2(t) \rangle^{-1}$ [1], generalized synchronization can be extended from the classical to the quantum regime by considering conjugate quantities simultaneously, and the corresponding measure can be defined as

$$S_g(t) := \langle \hat{q}_{g-}^2(t) + \hat{p}_{g-}^2(t) \rangle^{-1}, \quad (3)$$

where $\hat{q}_{g-} := [h_1(\hat{q}_1) - h_2(\hat{q}_2)]/\sqrt{2}$ and $\hat{p}_{g-} := [h_1(\hat{p}_1) - h_2(\hat{p}_2)]/\sqrt{2}$ are the quantized generalized error operators.

Nevertheless, it is not easy to use Eq. (3) directly in a concrete model. In some cases, $h_{1,2}(q, p_{1,2})$ are not strict physical descriptions because they are actually superoperators.

On the other hand, it could be difficult to calculate $S_g(t)$ in CV quantum systems. Therefore, in order to analyze quantum synchronization in CV mesoscopic systems, we adopt the mean-field approximation to simplify Eq. (3). The synchronization measure can then be divided into two parts: the first-order criterion describes the consistency of expectation values:

$$\begin{aligned} \lim_{t \rightarrow \infty} |h_1(q_1(t)) - h_2(q_2(t))| &\rightarrow 0, \\ \lim_{t \rightarrow \infty} |h_1(p_1(t)) - h_2(p_2(t))| &\rightarrow 0, \end{aligned} \quad (4)$$

and the second-order measure determines quantum fluctuations:

$$S'_g(t) := \langle \delta q_{g-}^2(t) + \delta p_{g-}^2(t) \rangle^{-1}, \quad (5)$$

where o refers to $\langle o \rangle$ and $\delta o := \hat{o} - o$ for $o \in \{q_{g-}, p_{g-}\}$.

The physical meanings of Eqs. (4) and (5) are can better explain quantum synchronization, i.e., the systems' expectation values are required to satisfy the "classical" generalized synchronization conditions, and the perturbation on synchronization behavior caused by the quantum effect is squeezed as much as possible. To verify this, Eq. (5) will be equivalent to Eq. (3) if the first-order criterion is satisfied. Conversely, if a designed external field can not only cause the evolutions of the systems to realize "classical" generalized synchronization conditions, but also increase the corresponding second-order measure S'_g , then it can be thought of as an appropriate control field for realizing quantum synchronization. This is the basic idea of designing the control field.

In some particular models, if h_1 and h_2 are selected as flat mappings, Eq. (5) can be further simplified to measure fluctuation,

$$S'_g(t) := \langle \delta q_-^2(t) + \delta p_-^2(t) \rangle^{-1}. \quad (6)$$

Here $q_- := (q_1 - q_2)/\sqrt{2}$ and $p_- := (p_1 - p_2)/\sqrt{2}$. Compared with Eq. (5), Eq. (6) is easier to obtain via the covariance matrix of the system.

III. LYAPUNOV-BASED SYNCHRONIZATION IN AN OPTOMECHANICAL SYSTEM

We analyze Lyapunov-based synchronization in an optomechanical system in order to explain more intuitively the theory of quantum generalized synchronization. Our model consists of two oscillators that couple with a Fabry-Pérot cavity together (see Fig. 1). The Hamiltonian corresponding to this model can be divided into four parts: $H = H_0 + H_{\text{int}} + H_{\text{div}} + H_c(t)$. Here $H_0 = \omega_l a^\dagger a + \sum_{j=1,2} (\frac{\omega_{mj}}{2} \hat{p}_j^2 + \frac{\omega_{mj}}{2} \hat{q}_j^2)$ is a sum of free Hamiltonians corresponding to the optical field and two oscillators. Moreover, $H_{\text{int}} = -g_1 a^\dagger a \hat{q}_1 - g_2 a^\dagger a \hat{q}_2$ and $H_{\text{div}} = iE(a^\dagger e^{-i\omega_l t} - a e^{i\omega_l t})$ are the standard forms of optomechanical interaction and driving field, respectively [30,31]. $H_c(t)$ is an external control Hamiltonian that represents the coupling with a designed time-dependent field. Here we consider a form of the control field that can create a deviation in the potential terms of two oscillators. This effect can be regarded as a time-dependent rescaling of the mirror frequency [32], i.e.,

$$\frac{\omega_{mj}}{2} \hat{q}_j^2 \rightarrow \frac{\omega_{mj}}{2} [1 + C_j(t)] \hat{q}_j^2. \quad (7)$$

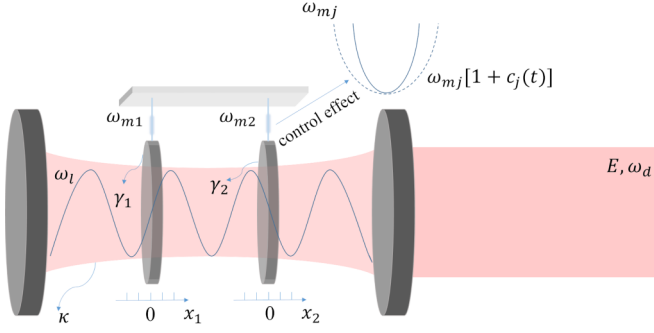


FIG. 1. Diagram of an optomechanical system corresponding to our model. Two oscillators are placed at the wave nodes of a Fabry-Pérot cavity, and they couple with the cavity field via linear optomechanical interactions. Their origins are set at the equilibrium positions.

We will present a more detailed discussion about how to realize this form of control field using specific experiments in Sec. V. The Hamiltonian of the whole system is written as follows after a frame rotating:

$$H = \sum_{j=1,2} \left\{ \frac{\omega_{mj}}{2} \hat{p}_j^2 + \frac{\omega_{mj}}{2} [1 + C_j(t)] \hat{q}_j^2 - g_j a^\dagger \hat{a} \hat{q}_j \right\} - \Delta a^\dagger a + iE(a^\dagger - a). \quad (8)$$

In the above expression, a (a^\dagger) is the annihilation (creation) operator for the optical field, and for $j = 1, 2$, q_j and p_j are dimensionless position and momentum operators of the oscillator j , respectively. $\Delta = \omega_d - \omega_l$ refers to the detuning between the frequencies of the laser drive and the cavity mode, ω_{mj} is the mechanical frequency, g_j is the optomechanical coupling constant, and E is the drive intensity. To solve the dynamics of the system, we consider the dissipative effects in the Heisenberg picture, and we write the quantum Langevin equations as follows [32–34]:

$$\begin{aligned} \partial_t a &= (-\kappa + i\Delta)a + ig_1 a \hat{q}_1 + ig_2 a \hat{q}_2 + E + \sqrt{2\kappa} a^{\text{in}}, \\ \partial_t \hat{q}_j &= \omega_{mj} \hat{p}_j, \\ \partial_t \hat{p}_j &= -\omega_{mj} [1 + C_j(t)] \hat{q}_j - \gamma_j \hat{p}_j + g_j a^\dagger a + \hat{\xi}_j. \end{aligned} \quad (9)$$

Here κ is the decay rate of the optical cavity, and γ_j is the mechanical damping rate of each oscillator. a^{in} is the radiation vacuum input noise with the autocorrelation function $\langle a^{\text{in}}(t) a^{\text{in}\dagger}(t') \rangle = \delta(t - t')$ under a zero-temperature assumption [35]. Similarly, $\hat{\xi}_j(t)$ is the Brownian noise operator, which describes the dissipative friction force acting on the j th mirror. In the Markovian approximation, the autocorrelation function of $\hat{\xi}_j(t)$ satisfies the following relation: $\langle \hat{\xi}_j(t) \hat{\xi}_j(t') + \hat{\xi}_j(t') \hat{\xi}_j(t) \rangle / 2 = \gamma_j (2\bar{n}_b + 1) \delta_{jj} \delta(t - t')$, where $\bar{n}_b = [\exp(\hbar\omega_j/k_B T) - 1]^{-1}$ is the mean phonon number of the mechanical bath that gauges the temperature T [36–38]. (In Figs. 2 and 4, since we only consider the situation $\omega_{m1} \simeq \omega_{m2}$, the parameter n_b can be safely taken to be equal for both oscillators.)

Solving directly a set of nonlinear differential operator equations such as Eq. (9) is quite difficult, however a mean-field approximation is acceptable in our mesoscopic optomechanical model [31,39,41,42]. On the other hand, as

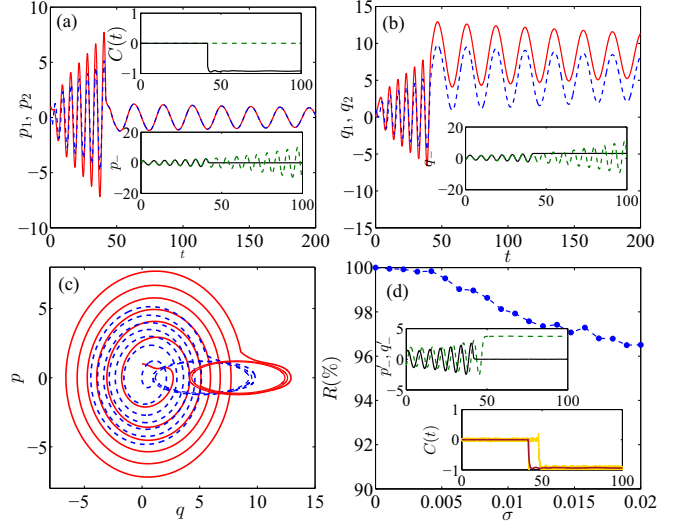


FIG. 2. Evolution of the expectation values (blue dashed and red solid lines), the control field, and the errors (the black solid and green dashed lines indicate that the control field is imposed or removed, respectively). Parts (a) and (b) correspond to the momentum and position operators of each oscillator, respectively. Here we set $\Delta = 1$ as a unit, and the other parameters are $\omega_{m1} = 1$, $\omega_{m2} = 1.005$, $g_1 = 0.008$, $g_2 = 0.005$, $E = 10$, $\kappa = 0.15$, $\gamma = 0.005$, and $\bar{n}_b = 0.05$. For the control field, the parameters are taken as $k = 2$ and $c_- = 3$. (c) The limit cycles of two oscillators in phase space. (d) The robustness of our controlled system. Here none of the simulations except for $R(\sigma)$ contain any noise. The bottom inset in (d) is the contrast of control fields without (red, dark) and with noise (yellow, pale), and the upper inset in (d) is the synchronization errors p'_- (black solid) and q'_- (green dashed) when the control field has noise. The horizontal axes of all the insets are the time t .

we discussed in Sec. II, the quantum synchronization measure modified by the mean-field approximation can describe the generalized synchronization effect more accurately. Therefore, every operator in Eq. (9) can be rewritten, respectively, as a sum of its expectation value and a small fluctuation near the expectation value, that is, $a(t) = A(t) + \delta a(t)$, $\hat{o}(t) = o(t) + \delta o(t)$, and $o \in (q_{1,2}, p_{1,2})$. Note that $\langle \delta a \rangle = 0$ and $\langle \delta o \rangle = 0$ under this definition. After neglecting the high-order fluctuation terms, the “classical” properties of our optomechanical system can be described by the following nonlinear equations:

$$\begin{aligned} \partial_t A &= (-\kappa + i\Delta)A + ig_1 A q_1 + ig_2 A q_2 + E, \\ \partial_t q_j &= \omega_{mj} p_j, \\ \partial_t p_j &= -\omega_{mj} [1 + C_j(t)] q_j - \gamma_j p_j + g_j |A|^2, \end{aligned} \quad (10)$$

and the corresponding quantum fluctuations can also be confirmed by

$$\begin{aligned} \partial_t \delta a &= (-\kappa + i\Delta) \delta a + \sum_{j=1,2} ig_j (q_j \delta a + A \delta q_j) + \sqrt{2\kappa} a^{\text{in}}, \\ \partial_t \delta q_j &= \omega_{mj} \delta p_j, \\ \partial_t \delta p_j &= -\omega_{mj} [1 + C_j(t)] \delta q_j - \gamma_j \delta p_j \\ &\quad + g_j (A^* \delta a + A \delta a^\dagger) + \hat{\xi}_j, \end{aligned} \quad (11)$$

transforming the annihilation operators to the forms of $a = (\hat{x} + i\hat{y})/\sqrt{2}$ and $a^{\text{in}} = (\hat{x}^{\text{in}} + i\hat{y}^{\text{in}})/\sqrt{2}$, respectively. Equation (11) can then be rewritten more concisely as $\partial_t \hat{u} = S\hat{u} + \hat{\zeta}$ by setting the vectors $\hat{u} = (\delta x, \delta y, \delta q_1, \delta p_1, \delta q_2, \delta p_2)^\top$ and $\hat{\zeta} = (\hat{x}^{\text{in}}, \hat{y}^{\text{in}}, 0, \hat{\xi}_1, 0, \hat{\xi}_2)^\top$, and the corresponding S is a time-dependent coefficient matrix (see Appendix for more details). In this representation, the evolution of the correlation matrix D , defined as

$$D_{ij}(t) = D_{ji}(t) = \frac{1}{2} \langle \hat{u}_i(t) \hat{u}_j(t) + \hat{u}_j(t) \hat{u}_i(t) \rangle, \quad (12)$$

can be derived directly by (see [15,39,41,42])

$$\partial_t D = SD + DS^\top + N. \quad (13)$$

N is a noise matrix that will be in diagonal form, i.e., $\text{diag}(\kappa, \kappa, 0, \gamma_1(2\bar{n}_b + 1), 0, \gamma_2(2\bar{n}_b + 1))$, if the noise correlation is defined by $\langle \hat{\zeta}_i(t) \hat{\zeta}_j(t') + \hat{\zeta}_j(t) \hat{\zeta}_i(t') \rangle / 2 = N_{ij} \delta(t - t')$. With the help of Eq. (13), the above-mentioned synchronization measure S'_g can be simply expressed as

$$\begin{aligned} S'_g(t) &= \langle \delta q_-^2(t) + \delta p_-^2(t) \rangle^{-1} \\ &= \left\{ \frac{1}{2} [D_{33}(t) + D_{55}(t) - 2D_{35}(t)] \right. \\ &\quad \left. + \frac{1}{2} [D_{44}(t) + D_{66}(t) - 2D_{46}(t)] \right\}^{-1}, \quad (14) \end{aligned}$$

and its evolution can be obtained by solving Eqs. (10) and Eq. (13) in order. At this point, all the dynamic properties of our system, including synchronization and correlation, can be learned by means of the solutions of Eqs. (10), (13), and (14). In the following subsections, we introduce two common forms of generalized synchronization, namely constant error synchronization (Sec. III A) and time-delay synchronization (Sec. III B), to exhibit our ability with regard to control synchronization. We will also prove how the controller is designed in order to realize these synchronizations. In a general discussion of synchronization, controlled systems may be arbitrary and have certain differences. These differences may mean that the amplitudes of the two systems are not fixed values but take on small oscillations with time evolution. For definiteness and without loss of generality, we will impose the control field at different stages for different generalized synchronizations, that is, we start imposing the control field when the system is unstable and is at the initial stage of evolution of constant error synchronization. However, for time-delay synchronization, we will impose the control field after the system reaches its steady state without the control field.

A. Constant error synchronization

Constant error synchronization can be regarded as a translation in phase space between two systems. In Eq. (2), if we let $h_1(x_1) = x_1 + c_1$ and $h_2(x_2) = x_2 + c_2$, the ‘‘classical’’ synchronization criterion will be

$$\lim_{t \rightarrow \infty} |x_1(t) - x_2(t)| \rightarrow c_2 - c_1 = c_-, \quad (15)$$

where c_- is the so-called constant error. In view of the direct influence of the controller on $\partial_t p_j$, at first we only consider the evolutions of the momentum operators, and further construct the following Lyapunov function by using their expectation

values:

$$V_p(t) = [p_1(t) - p_2(t)]^2. \quad (16)$$

One can easily verify that $V_p(t)$ meets the conceptual requirements of a Lyapunov function, i.e., $V_p \geq 0$, and $V_p = 0$ is valid only when $p_1(t) - p_2(t) = 0$. Substituting Eq. (10) into Eq. (16), the time derivative of V_p can be calculated handily if $C_1(t) = C_2(t) = C(t)$,

$$\begin{aligned} \dot{V}_p(t) &= 2[\dot{p}_1(t) - \dot{p}_2(t)][p_1(t) - p_2(t)] \\ &= 2\{[1 + C(t)](\omega_{m2}q_2 - \omega_{m1}q_1) - \gamma_1 p_1 \\ &\quad + \gamma_2 p_2 + (g_1 - g_2)|A|^2\}(p_1 - p_2). \quad (17) \end{aligned}$$

We find that $\dot{V}_p(t)$ is always nonpositive by setting

$$\dot{p}_1(t) - \dot{p}_2(t) = -k[p_1(t) - p_2(t)], \quad (18)$$

where k is a positive real number. With this choice, V_p simultaneously satisfies $V_p \geq 0$ and $\dot{V}_p = -2k[p_1(t) - p_2(t)]^2 \leq 0$. Under this condition, the system will gradually evolve to a stable state that corresponds to the origin of the Lyapunov function, i.e., $p_1(t) = p_2(t)$ [27]. To satisfy the required form of the Lyapunov function, the control field can be obtained based on Eqs. (17) and (18),

$$C(t) = \frac{(\gamma - k)[p_1 - p_2] - (g_1 - g_2)|A|^2}{\omega_{m2}q_2 - \omega_{m1}q_1} - 1, \quad (19)$$

where we have already set $\gamma_1 = \gamma_2 = \gamma$. To avoid confusion in the following discussion on time-delay synchronization, it must be emphasized that all mechanical quantities that are not specifically marked in this equation represent the expectation values at time t [e.g., $p_1 := p_1(t)$].

We notice, however, that the control field $C(t)$ in Eq. (19) could be infinite when the tracks of q_1 and q_2 are adjacent. In particular, complete synchronization is not acceptable if $\omega_{m1} \simeq \omega_{m2}$. To avoid this singularity, it is necessary to add a lower bound in the denominator of the control field. Therefore, the control field is modified as follows:

$$C(t) = \begin{cases} \frac{(\gamma - k)[p_1 - p_2] - (g_1 - g_2)|A|^2}{\omega_{m2}q_2 - \omega_{m1}q_1} - 1 \\ \quad (\text{when } |\omega_{m2}q_2 - \omega_{m1}q_1| > c_-), \\ 0 \\ \quad (\text{when } |\omega_{m2}q_2 - \omega_{m1}q_1| \leq c_-). \end{cases} \quad (20)$$

The physical mechanism corresponding to Eq. (20) can be interpreted as follows: Assuming that the gap between two oscillators is small enough to satisfy $|\omega_{m2}q_2 - \omega_{m1}q_1| \leq c_-$ at the initial moment, the control field will not work and the difference between oscillators under different Hamiltonians will increase; once such a difference crosses the boundary $|\omega_{m2}q_2 - \omega_{m1}q_1| > c_-$, a nonzero control field will drag their orbits close to each other until a critical distance is reached, which will cause the invalid control field to resume. As time passes, the error evolution will be controlled in a stable limit ellipse. Under a particular k and c_- , it can be regarded as a fixed point if the major axis of this ellipsoid is small enough. In this case, two systems will finally realize such a synchronization: $p_1 - p_2 = 0$ and $q_1 - q_2 = c_-$. Therefore, we make sure that

$C(t)$ in Eq. (19) is able to control the system, thus generalized synchronization is achieved.

In Fig. 2, we provide simulation results of the two oscillators to verify the synchronization phenomenon under the control field. In Fig. 2(a), one can directly see that the momenta of two oscillators will take on consistent evolution after $t = 41.3$, which is exactly what happens with the time point at which the control field is nonzero. Correspondingly, the momentum error will stabilize at zero instead of generally enlarging along with the control field. Figure 2(a) also shows quantitatively that the control field is a slowly varying function of time. Such a slowly varying control field can improve the stability of the system, and at the same time it is easier to implement in experiments. In Fig. 2(b), we plot the positions of two oscillators and the corresponding error. It illustrates that, although two oscillators are not consistent in their positions, the error can still maintain a constant (c_-). Taking Figs. 2(a) and 2(b) together, we can determine that constant error synchronization between two oscillators has been achieved. In Fig. 2(c), we show the “tracks” of two oscillators in phase space. Two oscillators will evolve to their respective limit cycles, and, as we predicted above, constant error synchronization corresponds to a translation between the limit cycles in phase space. Figure 2(d) illustrates the robustness of our synchronization system. Here we assume that each quantity in Eq. (20) has had a Gaussian noise added whose standard deviation is σ , i.e., $o(t) = \mathcal{N}(o(t), \sigma)$ ($o \in \{q_{1,2}, p_{1,2}, A\}$), and the final control field also has a noise [$C(t) = \mathcal{N}(C(t), \sigma)$] when it is imposed on the system. The accuracy of the synchronization scheme in this case is described by the following auxiliary quantity:

$$R(\sigma) = 1 - \frac{[(q_- - q'_-)^2 + (p_- - p'_-)^2]^{1/2}}{\sqrt{2}r}. \quad (21)$$

In this expression, p'_- and q'_- (p_- and q_-) refer to the synchronization errors when the control field has (does not have) a Gaussian noise, and r is the average radius of the limit cycle. One can find that $R(\sigma)$ will always remain above 96% even if $\sigma = 0.02$. Under the above parameters, even if there are obvious fluctuations in the control field, the errors between two oscillators are still stable upon approaching 0 and c'_- . Therefore, we confirm that our control is stable enough for some interferences.

In addition to the expectation value, Mari’s measure is also calculated to prove that quantum fluctuation is similarly squeezed by the control field. Figure 3(a) illustrates that an increasing S'_g substitutes the trend to 0, which significantly outperforms the uncontrolled situation. Therefore, we recognize that the control field can indeed achieve quantum control rather than the synchronization of the classical level. To compare our generalized synchronization with some other complete synchronizations, in the inset in Fig. 3(a) we calculate S_g by using classical errors and S'_g because S_g is of the same physical meaning as the synchronization measure in Ref. [1]. It can be found that $S_g \leq S'_g$ because the classical error information is also included in S'_g . In Fig. 3(b), we also show how the bath temperature will influence the synchronization phenomenon. Here we calculate the time-averaged synchronization measure, i.e., $\bar{S}_g = [\int_0^T S_g(t) dt]/T$, with varied bath temperature. It is known that $S'_g(t)$ will remain almost unchanged if the bath

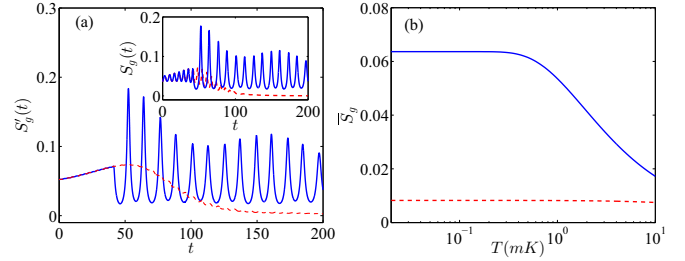


FIG. 3. (a) Evolutions of the modified synchronization measure S'_g . The inset in (a) shows the evolutions of the synchronization measure S_g . (b) Time-averaged synchronization measures with varied bath temperature. Blue (solid) lines correspond to the imposed control field, and red (dotted) lines denote that the case control field disappears. In these simulations we set $T = 200$, and other parameters are the same as those in Fig. 2.

temperature is limited within 1 mK ($\bar{n}_b = 0.28$ corresponding to a MHz phonon frequency), and it is still larger than that belonging to the uncontrolled system even though T goes up to 10 mK ($\bar{n}_b = 6.14$). This range is quite broad compared to other correlation control schemes in optomechanical systems [43,44].

B. Time-delay synchronization

Time-delay synchronization can be regarded as a constant phase deviation between two systems, and the “tracks” in phase space are overlapping like complete synchronization. In Eq. (2), if we set $h_1(x_1) = x_1(t)$ and $h_2(x_2) = x_2(t - \tau)$, the “classical” synchronization criterion will be

$$\lim_{t \rightarrow \infty} |x_1(t) - x_2(t - \tau)| \rightarrow 0. \quad (22)$$

Similar to the above discussions, we define the following Lyapunov function:

$$V_p(t) = [p_1(t) - p_2(t - \tau)]^2, \quad (23)$$

and its derivative can also be expressed as $\dot{V}_p = 2[\dot{p}_1 - \dot{p}_2(t - \tau)][p_1 - p_2(t - \tau)]$, where

$$\begin{aligned} \dot{p}_1 - \dot{p}_2(t - \tau) = & -\omega_m[1 + C_1]q_1 - \gamma_1 p_1 + g_1|A|^2, \\ & + \omega_m q_2(t - \tau) + \gamma_2 p_2(t - \tau) \\ & + g_2|A(t - \tau)|^2. \end{aligned} \quad (24)$$

It must be emphasized again that, in the above expressions, all the mechanical quantities not specifically marked represent the expectation values at time t . Similarly, we set

$$\dot{p}_1 - \dot{p}_2(t - \tau) = -k[p_1(t) - p_2(t - \tau)] \quad (25)$$

to satisfy $V_p \geq 0$ and $\dot{V}_p = -2k[p_1 - p_2(t - \tau)]^2 \leq 0$. Then the corresponding control field will become

$$C_1(t) = \frac{(\gamma - k)[p_1 - p_2(t - \tau)] - g_1|A|^2 + g_2|A(t - \tau)|^2 - \omega_{m2}q_2(t - \tau)}{-\omega_{m1}q_1} - 1 \quad (26)$$

by setting $C_2(t) = 0$ and $\gamma_1 = \gamma_2 = \gamma$ for simplicity.

Equation (26) is also of a singular point at $q_1(t) = 0$, therefore an artificial boundary is necessary to avoid an infinite control field, too. Unlike Eq. (20), our purpose here is to make two systems achieve complete synchronization after eliminating the time delay. Therefore, this limitation works on the whole control field instead of the denominator. So the control field should be [40]

$$C_1(t) = \begin{cases} \frac{(\gamma - k)[p_1 - p_2(t - \tau)] - g_1|A|^2 + g_2|A(t - \tau)|^2 - \omega_{m2}q_2(t - \tau)}{-\omega_{m1}q_1} - 1 & (-C_M \leq C_1 \leq C_M), \\ C_M & (C_1 > C_M), \\ -C_M & (C_1 < -C_M). \end{cases} \quad (27)$$

In Figs. 4(a) and 4(b), we show that the evolutions of one oscillator seem to be a time translation of the other oscillator, and the errors tend to zero like complete synchronization after eliminating the time delay. Figure 4 also exhibits a quickly varying control field that is different with the performance in constant error synchronization. In general, a quickly varying control field can make the system achieve synchronization faster. Figures 4(a) and 4(b) show that two oscillators will achieve synchronization in a short period of time, $t < 10$, and synchronization time is reduced fourfold compared with that

in Figs. 2(a) and 2(b). Furthermore, Fig. 4(d) illustrates that synchronization accuracy is 99%, which means robustness is enhanced because we start the control field from a steady state. We also plot the limit cycles of two oscillators in Fig. 4(c). It is known that two limit cycles are almost coincident most of the time except at short time intervals at the origin and destination points at which both limit cycles take on inconsistent evolutions because of the time delay.

We also consider the evolutions of quantum fluctuation and synchronization measure S_g . Figure 5(a) shows that after adding the control field, S_g is significantly larger than zero even though the control field is not imposed until the system reaches steady state after a long time evolution. Simultaneously considering Figs. 3 and 5, we think that our control has no special requirements for the initial state of the system, and the control field can be imposed at any time in our model. Figure 5(b) also illustrates that the destruction of the synchronization effect caused by the environment is also weakened, and $\bar{S}'_g(t)$ will still remain at a high level even at $T = 10$ mK. From this perspective, we believe that quickly varying the control field is also an appropriate form of synchronization control.

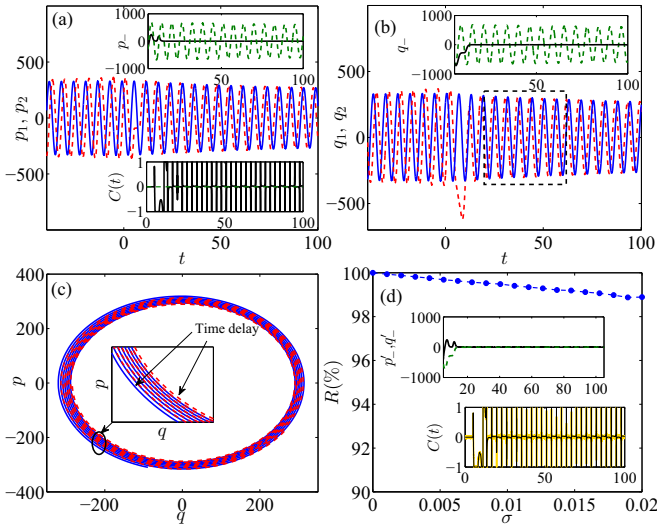


FIG. 4. Evolutions of the expectation values (blue dashed and red solid lines), the control field, and the errors (black solid and green dashed lines indicate that the control field is imposed or removed, respectively). Parts (a) and (b) correspond to the momentum and position operators of each oscillator, respectively. (c) The limit cycles of two oscillators in phase space. This phase diagram corresponds to the curve segment within the black dotted box in (b). (d) The robustness of the control system. Here we set $\tau = 5$, $C_M = 1$, and the other parameters are the same as those in Fig. 2. The bottom inset in (d) is the contrast of the control field without (red, dark) and with noise (yellow, pale), and the upper inset in (d) is the synchronization errors p'_- (black solid) and q'_- (green dashed) when the control field has noise. The horizontal axes of the insets in (a), (b), and (d) are the time t . Here we define the moment imposing the control field as $t = 0$.

IV. CORRELATION IN GENERALIZED SYNCHRONIZATION

The correlation between synchronized quantum systems is an important topic of research in QIP. Intuitively, two different systems can achieve consistency to some extent, meaning

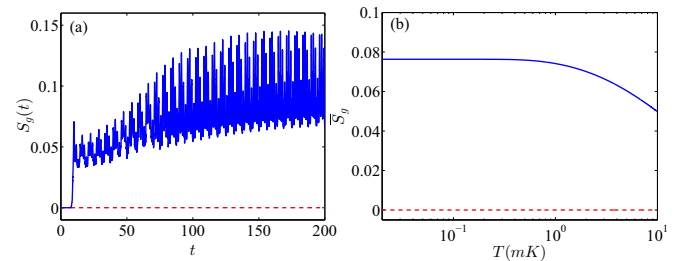


FIG. 5. (a) Evolutions of the modified synchronization measure. (b) Time-averaged synchronization measures with varied bath temperature. Blue (solid) lines correspond to the imposed control field, and red (dotted) lines indicate that the control field disappears. Here all parameters are the same as those in Fig. 3.

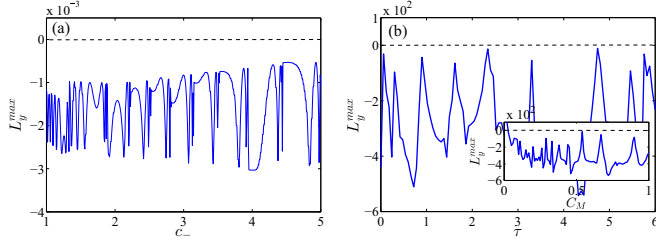


FIG. 6. The largest Lyapunov exponents of the errors with varied c_- (a) and τ (b) corresponding to constant error synchronization and time delay synchronization, respectively. Here all the parameters except c_- and τ are the same as those in Fig. 2. The inset in (b) shows the largest Lyapunov exponents of the errors with varied C_M under $\tau = 5$.

that there inevitably exists a certain correlation between the systems. To verify this, quantum mutual information, which is a measure of total correlation, has been proved to have homology with synchronization measures in VdP oscillators [3]. However, it is very difficult to identify this type of correlation, especially because the existence of quantum entanglement in CV synchronization is controversial [1,3,8,14]. Therefore, we pay more attention to the properties of entanglement when we consider the quantum correlation in our model.

The mean-field approximation used above can make it more convenient to analyze classical correlation and quantum entanglement. The classical correlation can be verified by calculating the largest Lyapunov exponent of the errors, i.e., $L_y^{\max} = \max\{L_y(p_{g-}), L_y(q_{g-})\}$, where

$$L_y(o) = \lim_{t \rightarrow \infty} \frac{1}{t} \ln \left| \frac{\delta o(t)}{\delta o(0)} \right| \quad (o \in \{p_{g-}, q_{g-}\}). \quad (28)$$

Using the stability criterion, one can determine whether the system is stable by comparing L_y with 0 [41,47]. In particular, as we discussed in Ref. [15], the largest Lyapunov exponent of error can be regarded as a criterion of quantum synchronization, i.e., a positive L_y indicates that two systems are not synchronized, while a negative L_y means the ‘‘classical’’ parts of two systems are synchronized. On the other hand, CV quantum entanglement is measured by Gaussian negativity $E_n = \max\{0, -\log_2 v_-\}$ [34,48,49], where

$$v_- = \frac{\sqrt{\Delta(\Gamma)} - \sqrt{\Delta(\Gamma)^2 - 4 \det \Gamma}}{2}, \quad (29)$$

$\Delta(\Gamma) = \det A + \det B - 2 \det C$, and

$$\Gamma = \begin{pmatrix} D_{33} & D_{34} & D_{35} & D_{36} \\ D_{43} & D_{44} & D_{45} & D_{46} \\ D_{53} & D_{54} & D_{55} & D_{56} \\ D_{63} & D_{64} & D_{65} & D_{66} \end{pmatrix} = \begin{pmatrix} A & C \\ C^\top & B \end{pmatrix}. \quad (30)$$

In Fig. 6, we plot the largest Lyapunov exponents under different characteristic parameters (c_- , τ , and C_M). The results show that a negative Lyapunov exponent always emerges under different control fields. This performance is superior to our conclusion in Ref. [15], in which we found that the Lyapunov exponent corresponding to coupling synchronization is not always less than 0 under different parameters, but it depends sensitively on varying the coupling intensity between two

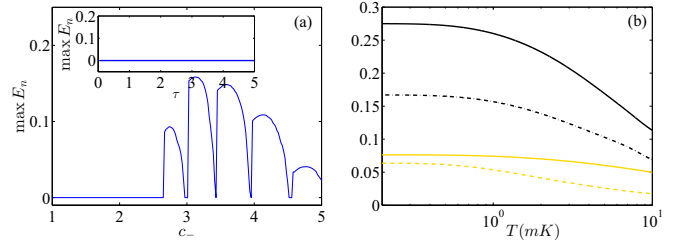


FIG. 7. (a) The maximum negativities of the errors with varied c_- (a) and τ and C_M (b) corresponding to constant error synchronization and time-delay synchronization, respectively. Here all parameters except c_- , τ , and C_M are the same as those in Fig. 2. (b) Time-averaged synchronization measures with varied bath temperature. Here the black (dark) lines correspond to complete synchronization (solid line) and phase synchronization (dotted line) in Ref. [1], respectively. The yellow (pale) lines correspond to our constant error synchronization (dotted line) and time-delay synchronization (solid line).

optomechanical systems. This means, compared to the direct coupling between two systems, that the designed Lyapunov function can more effectively help the systems to establish correlation at the expected value level.

In Fig. 7(a), we plot the results of maximum negativity under different characteristic parameters. It should be noted that generalized synchronization is actually a necessary condition for complete synchronization, and the characteristic parameters can be regarded as a description of the gap between generalized synchronization and complete synchronization. Consequently, one can compare complete synchronization with generalized synchronization by setting $c_- \rightarrow 0$, $\tau \rightarrow 0$, and $C_M \rightarrow \infty$. Figure 7(a) shows that quantum entanglement does not exist until $c_- = 2.65$, at which point it takes on the oscillating variation, and its maximum value is at $c_- = 3.13$. The evolution of maximum implies that when c_- tends to 0, the oscillators are equivalent to achieving complete synchronization and they are always separable in this case. In the range of generalized synchronization, however, the entanglement appears at specific c_- . The inset of Fig. 7(a) shows that the entanglement will be hard to achieve if we do not control our scheme until the system reaches steady state. This conclusion suggests that, compared with generating entanglement by a local control field, it is better to achieve entangled synchronization by making the system quickly reach synchronization before the environment destroys entanglement.

In Fig. 7(b), we contrast S_g with S_c and S_p , which are calculated and reported in Ref. [1], to measure complete synchronization and phase synchronization between two coupled optomechanical systems. We find that S_g in our scheme is smaller than S_c and S_p because generalized synchronization cannot ensure that the dynamical variables of the two systems are completely equal. Quantitatively, the most perfect synchronization effect we can achieve is equivalent to the phase synchronization in Ref. [1] under $T = 8$ mK. In other words, the compressing effect for the difference between quantum fluctuations in complete synchronization and phase synchronization is better than that in our generalized synchronization. Nevertheless, as we discussed above, the

generalized synchronization is a more flexible synchronization. Even though the entanglement is hindered by complete synchronization and phase synchronization in some models or parameters [1,3], one can always relax some restrictions by designing different generalized synchronizations to ensure that entanglement can coexist with synchronization. Therefore, we think that our generalized synchronization is also a suitable resource for QIP.

V. DISCUSSION AND RESULTS

Here we present a brief discussion about the parameters of our optomechanical system and the realization scheme of the control field. The parameters selected in the simulations are similar to those in Refs. [1,14,39,45,46]. However, in order to highlight the roles of the coupling and the controller, we appropriately reduce the value of the driving intensity [15]. Beyond that, the deviation in potential such as that in Eq. (7) has been investigated by theoretical research [32], and recent works reported that the deviation can be achieved by using charged mechanical resonators [50–53]. For example, Zhang considered a charged mechanical resonator (MR) that couples to two identical electrodes via the Coulomb interaction. In this model, the MR will have an effective frequency $\omega_{\text{eff}} = \omega_m \sqrt{1 + \eta f(t)}$, where

$$\eta = \frac{C_0 U_0 Q_{\text{MR}}}{\pi \epsilon_0 m \omega_m^2 d^3} \quad (31)$$

is obtained in Ref. [52]. If the voltage is set as $U(t) = C(t)U_0/\eta$, the effective frequency will become $\omega_{\text{eff}} = \omega_m \sqrt{1 + C(t)}$ and Eq. (7) can be achieved. Therefore, the control field can be realized by only regulating the bias gate voltage, and we are sure that the control terms in Eqs. (20) and (27) can be achieved easily in experiments. Using the same circuit parameters as those in Ref. [52], we find that our control field corresponds to $U_0 = 7.00$ V and $f(t) \sim 10^{-5}$. It has already been proven in Ref. [52] that the oscillator noise is derived mainly from environmental noise in the range $f(t) \in [10^{-10}, 10^0]$. Therefore, we think that the quantum noise from the control field itself can be neglected in this case.

Here we analyze how strongly the neglected quantum effects can influence the dynamics discussed above. For the strict solution of Eq. (8), the mechanical equations of the system are open due to the nonlinear term $g_j a^\dagger a \hat{q}$ in the Hamiltonian. Let us reexamine the derivation process from Eq. (9) to Eqs. (10) and (11). Equation (10) can be obtained after neglecting the terms $i g_j \langle \delta a \delta q_j \rangle$ and $g_j \langle \delta a^\dagger \delta a \rangle$ because we assume $\langle \delta o_1 \delta o_2 \rangle = \langle \delta o_1 \rangle \langle \delta o_2 \rangle$ ($o_1, o_2 \in \{a, a^\dagger, q_j\}$). To obtain Eq. (11), the terms $g_j \delta a \delta q_j$ and $g_j \delta a^\dagger \delta a$ have also been ignored since they are high-order small quantities if there are a large number of phonons in the oscillators. It is worth noting that all the ignored terms impact the dynamics of the system with interaction factor g_j , and the quantum correlation may disappear with large κ . Therefore, in addition to the phonon number and the bath temperature, the accuracy of the approximation is also related to the “quantum parameter” g_j/κ , which is defined in Refs. [54,55]. It has been proven in Ref. [54] that the system will correspond to the classical limit even if the phonon number is not very large, and

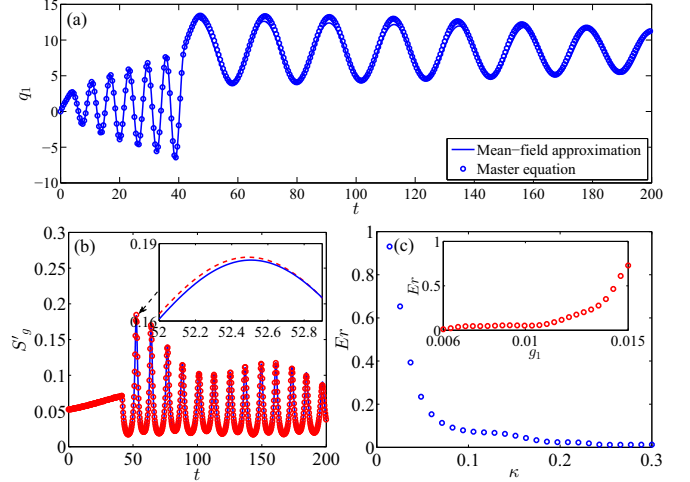


FIG. 8. Comparison of two computation methods corresponding to the linear mean-field approximation and the nonlinear quantum master equation. (a) Evolutions of expectation values q_1 . (b) Evolutions of S'_g . (c) Relative error as a function of κ under $g_1 = 0.008$. The inset in (c) shows the relative error as a function of g_1 under $\kappa = 0.15$. The other parameters are the same as those in Fig. 2.

the bath temperature is low when the quantum parameter vanishes. Correspondingly, increasing the quantum parameter will enhance the quantum effects on the motion of the system. In the simulations of two kinds of synchronizations, the quantum parameters are set as $g_1/\kappa \sim 0.05$ and $g_2/\kappa \sim 0.03$. We think that the expected values and the first-order fluctuation of the system can be described accurately by Eqs. (10), (11), and (13).

To verify the above discussion, we utilize the quantum master equation to calculate the expected values and S'_g . Using the quantum master equation, we calculate all the first-order nonlinear terms strictly, and we only ignore the correlation between second-order nonlinear terms [56]. We find that the constant error synchronization has a minimum phonon number. Therefore, we focus here on the damage inflicted by the high-order nonlinear terms on the mean-field approximation corresponding to Fig. 2. In Fig. 8, we plot a comparison of these two methods, and we show that the influence of the first-order nonlinear terms is quite small under our parameters. Considering the fact that first-order nonlinear terms have almost no impact on the system, the higher-order nonlinear terms should also have no effect on the system. A similar conclusion is also verified in Fig. 8(b), which shows an almost unchanged synchronization measure S'_g . To quantitatively illustrate this problem, we also calculate the relative deviation between expected values, which is defined as $Er = [\int_0^T |q_1(t) - q_1'(t)| dt] / Tr'$. Here q_1 and q_1' correspond to the expected values of \hat{q}_1 calculated by the mean-field approximation and the master equation, respectively, and r' is the average radius of the limit cycle [the same definition as in Eq. (21)] calculated by the master equation. In Fig. 8(c), we find that the first-order nonlinear terms neglected by the mean-field approximation can only produce a deviation of less than 5%, but this deviation will increase significantly when g_1 increases or κ decreases. Generally speaking, the

mean-field approximation will become more applicable in high bath temperature. Because all the above results are calculated in low temperature ($\bar{n}_b = 0.05$), we think that the mean-field approximation is available in our simulations due to small g_j/κ . Moreover, it can be seen from Figs. 3(b) and 5(b) that the synchronization performance will be disturbed by high bath temperature. To sum up, one necessary condition of our scheme is that g_j/κ should be small enough to ensure that the mean-field approximation works in low temperature.

In summary, we have extended Mari's theories about quantum complete synchronization and phase synchronization to a more general situation, defined as quantum generalized synchronization in this paper. The corresponding control methods, criteria, and measures are also proposed quantitatively based on the Lyapunov function, the Lyapunov exponent, and a modified Mari measure. This generalized synchronization can be regarded as a prerequisite of traditional quantum synchronization, and it can establish a more flexible relation between two controlled systems. To verify this, we have demonstrated that some important properties in our model, such as entanglement in synchronization, are consistent with

previous works if the generalized synchronization tends to complete synchronization. Therefore, designers can complete different synchronizations according to their requirements based on our theory. To make our theory more intuitive, we have considered two common generalized synchronizations, that is, the so-called constant error synchronization and time-delay synchronization in an optomechanical system. With the help of control fields designed by the Lyapunov function, we have proved that two oscillators can satisfy the requirements of various synchronizations. We believe that our work brings a certain application value in quantum-information transmission, quantum control, and quantum logical processing.

ACKNOWLEDGMENTS

The authors thank Jiong Cheng, Wenzhao Zhang, and Yang Zhang for useful discussion. This research was supported by the National Natural Science Foundation of China (Grants No. 11175033 and No. 11574041) and the Central Universities (DUT13LK05).

APPENDIX: PARAMETERS IN QUANTUM LANGEVIN EQUATIONS

The concrete form of the coefficient matrix S in Eq. (13) is

$$S = \begin{pmatrix} -\kappa & -(\Delta + g_1q_1 + g_2q_2) & -\sqrt{2}g_1\text{Im}(A) & 0 & -\sqrt{2}g_2\text{Im}(A) & 0 \\ \Delta + g_1q_1 + g_2q_2 & -\kappa & \sqrt{2}g_1\text{Re}(A) & 0 & \sqrt{2}g_2\text{Re}(A) & 0 \\ 0 & 0 & 0 & \omega_{m1} & 0 & 0 \\ \sqrt{2}g_1\text{Re}(A) & \sqrt{2}g_1\text{Im}(A) & -\omega_{m1}[1 + c_1(t)] & -\gamma_1 & 0 & 0 \\ 0 & 0 & 0 & 0 & 0 & \omega_{m2} \\ \sqrt{2}g_2\text{Re}(A) & \sqrt{2}g_2\text{Im}(A) & 0 & 0 & -\omega_{m2}[1 + c_2(t)] & -\gamma_2 \end{pmatrix}. \quad (\text{A1})$$

[1] A. Mari, A. Farace, N. Didier, V. Giovannetti, and R. Fazio, *Phys. Rev. Lett.* **111**, 103605 (2013).
 [2] O. V. Zhirov and D. L. Shepelyansky, *Phys. Rev. B* **80**, 014519 (2009).
 [3] V. Ameri, M. Eghbali-Arani, A. Mari, A. Farace, F. Kheirandish, V. Giovannetti, and R. Fazio, *Phys. Rev. A* **91**, 012301 (2015).
 [4] M. H. Xu, D. A. Tieri, E. C. Fine, J. K. Thompson, and M. J. Holland, *Phys. Rev. Lett.* **113**, 154101 (2014).
 [5] M. H. Xu and M. J. Holland, *Phys. Rev. Lett.* **114**, 103601 (2015).
 [6] M. R. Hush, W. Li, S. Genway, I. Lesanovsky, and A. D. Armour, *Phys. Rev. A* **91**, 061401(R) (2015).
 [7] T. E. Lee and H. R. Sadeghpour, *Phys. Rev. Lett.* **111**, 234101 (2013).
 [8] T. E. Lee, C. K. Chan, and S. S. Wang, *Phys. Rev. E* **89**, 022913 (2014).
 [9] S. Walter, A. Nunnenkamp, and C. Bruder, *Phys. Rev. Lett.* **112**, 094102 (2014).
 [10] S. Walter, A. Nunnenkamp, and C. Bruder, *Ann. Phys. (Leipzig)* **527**, 131 (2015).
 [11] M. Samoylova, N. Piovella, G. R. M. Robb, R. Bachelard, and P. W. Courteille, [arXiv:1503.05616](https://arxiv.org/abs/1503.05616).
 [12] Y. Gul, [arXiv:1412.8497](https://arxiv.org/abs/1412.8497).
 [13] F. Quijandría, D. Porras, J. J. García-Ripoll, and D. Zueco, *Phys. Rev. Lett.* **111**, 073602 (2013).
 [14] L. Ying, Y.-C. Lai, and C. Grebogi, *Phys. Rev. A* **90**, 053810 (2014).
 [15] W. L. Li, C. Li, and H. S. Song, *J. Phys. B* **48**, 035503 (2015).
 [16] S. H. Choi and S. Y. Ha, *J. Phys. A* **47**, 355104 (2014).
 [17] G. Heinrich, M. Ludwig, J. Qian, B. Kubala, and F. Marquardt, *Phys. Rev. Lett.* **107**, 043603 (2011).
 [18] R. Lauter, C. Brendel, S. J. M. Habraken, and F. Marquardt, *Phys. Rev. E* **92**, 012902 (2015).
 [19] M. Zhang, G. S. Wiederhecker, S. Manipatruni, A. Barnard, P. McEuen, and M. Lipson, *Phys. Rev. Lett.* **109**, 233906 (2012).
 [20] M. Bagheri, M. Poot, L. Fan, F. Marquardt, and H. X. Tang, *Phys. Rev. Lett.* **111**, 213902 (2013).
 [21] M. H. Matheny, M. Grau, L. G. Villanueva, R. B. Karabalin, M. C. Cross, and M. L. Roukes, *Phys. Rev. Lett.* **112**, 014101 (2014).
 [22] M. Zhang, S. Shah, J. Cardenas, and M. Lipson, *Phys. Rev. Lett.* **115**, 163902 (2015).
 [23] Y. Xu, H. Wang, Y. Li, and B. Pei, *Commun. Nonlin. Sci. Numer. Simul.* **19**, 3735 (2014).

- [24] X. Wu, H. Wang, and H. Lu, *Nonlin. Anal.* **13**, 1441 (2012).
- [25] L. Lü, C. Li, L. Chen, and L. Wei, *Commun. Nonlin. Sci. Numer. Simul.* **19**, 2843 (2014).
- [26] T. Weiss, A. Kronwald, and F. Marquardt, *New J. Phys.* **18**, 013043 (2016).
- [27] G. Nicolis and I. Prigogine, *Self-organization in Nonequilibrium Systems* (Wiley, New York, 1977).
- [28] X. X. Yi, X. L. Huang, C. F. Wu, and C. H. Oh, *Phys. Rev. A* **80**, 052316 (2009).
- [29] S. C. Hou, M. A. Khan, X. X. Yi, D. Y. Dong, and I. R. Petersen, *Phys. Rev. A* **86**, 022321 (2012).
- [30] C. K. Law, *Phys. Rev. A* **51**, 2537 (1995).
- [31] M. Aspelmeyer, T. J. Kippenberg, and F. Marquardt, *Rev. Mod. Phys.* **86**, 1391 (2014).
- [32] A. Farace and V. Giovannetti, *Phys. Rev. A* **86**, 013820 (2012).
- [33] C. Genes, A. Mari, D. Vitalii, and S. Tombesi, *Adv. At. Mol. Opt. Phys.* **57**, 33 (2009).
- [34] Y. D. Wang and A. A. Clerk, *Phys. Rev. Lett.* **110**, 253601 (2013).
- [35] C. W. Gardiner and P. Zoller, *Quantum Noise* (Springer, Berlin, 2000).
- [36] V. Giovannetti and D. Vitali, *Phys. Rev. A* **63**, 023812 (2001).
- [37] Y. C. Liu, Y. F. Shen, Q. H. Gong, and Y. F. Xiao, *Phys. Rev. A* **89**, 053821 (2014).
- [38] X. W. Xu and Y. Li, *Phys. Rev. A* **91**, 053854 (2015).
- [39] A. Mari and J. Eisert, *Phys. Rev. Lett.* **103**, 213603 (2009).
- [40] Y. C. Liu, Y. F. Xiao, X. Luan, and C. W. Wong, *Phys. Rev. Lett.* **110**, 153606 (2013). To control the system, which has reached a steady state after long-time evolution, we also added a dissipative pulse to avoid the measure of an optical field.
- [41] G. L. Wang, L. Huang, Y. C. Lai, and C. Grebogi, *Phys. Rev. Lett.* **112**, 110406 (2014).
- [42] J. Larson and M. Horsdal, *Phys. Rev. A* **84**, 021804(R) (2011).
- [43] J. Q. Liao and F. Nori, *Phys. Rev. A* **88**, 023853 (2013).
- [44] W. Z. Zhang, J. Cheng, J. Y. Liu, and L. Zhou, *Phys. Rev. A* **91**, 063836 (2015).
- [45] M. Eichenfield, R. Camacho, J. Chan, K. J. Vahala, and O. Painter, *Nature (London)* **459**, 550 (2009).
- [46] M. Eichenfield, J. Chan, M. R. Camacho, K. J. Vahala, and O. Painter, *Nature (London)* **462**, 78 (2009).
- [47] Y. C. Lai and C. Grebogi, *Phys. Rev. E* **53**, 1371 (1996).
- [48] G. Adesso and F. Illuminat, *J. Phys. A* **40**, 7821 (2007).
- [49] C. Joshi, J. Larson, M. Jonson, E. Andersson, and P. Öhberg, *Phys. Rev. A* **85**, 033805 (2012).
- [50] Y. Li, L. A. Wu, and Z. D. Wang, *Phys. Rev. A* **83**, 043804 (2011).
- [51] P. C. Ma, J. Q. Zhang, Y. Xiao, M. Feng, and Z. M. Zhang, *Phys. Rev. A* **90**, 043825 (2014).
- [52] J. Q. Zhang, Y. Li, and M. Feng, *J. Phys: Condens. Matter* **25**, 142202 (2013). In this expression, Q_{MR} is the charge of the MR, and the two electrodes are separated by a distance $2d$. C_0 is the capacitance of the gate, $U(t) = U_0 f(t)$ is the tunable bias gate voltage, ϵ_0 is the vacuum dielectric constant, and m is the effective mass of MR.
- [53] X. Y. Lü, J. Q. Liao, L. Tian, and F. Nori, *Phys. Rev. A* **91**, 013834 (2015).
- [54] M. Ludwig, B. Kubala, and F. Marquardt, *New J. Phys.* **10**, 095013 (2008).
- [55] L. Bakemeier, A. Alvermann, and H. Fehske, *Phys. Rev. Lett.* **114**, 013601 (2015).
- [56] Terms such as $\langle a\hat{q}_1\hat{q}_1 \rangle$ are calculated strictly; only terms such as $\langle aa\hat{q}_1\hat{q}_1 \rangle$ are approximated as $\langle a\hat{q}_1 \rangle \langle a\hat{q}_1 \rangle$. Such a process can make the dynamic equations of the system closed, although the high-order nonlinearity causes them to open originally. Hence, the advantage of this method is that a cutoff on the density matrix is not needed when we simulate.